Femtosecond Double Proton-Transfer Dynamics in [2,2′-Bipyridyl]-3,3′-diol in Sol−Gel Glasses

P. Prosposito,† D. Marks, H. Zhang, and M. Glasbeek*

Laboratory for Physical Chemistry, University of Amsterdam, Nieuwe Achtergracht 129, 1018 WS Amsterdam, The Netherlands

Received: April 13, 1998; In Final Form: July 17, 1998

Intramolecular excited state double proton-transfer dynamics has been studied for [2,2′-bipyridyl]-3,3′-diol ($BP(OH)_2$) in sol−gel glass. By means of the femtosecond fluorescence up-conversion technique, the spectral dependence of the fluorescence transients obtained for $BP(OH)_2$ in a few sol−gel glasses has been followed. From the temporal behavior of the reconstructed spectra, two concurrent double proton-transfer pathways are concluded to occur in the sol−gel hosts: the first is a concerted double proton-transfer process (within 100 fs after the excitation pulse) and the second is a two-step process involving the reaction from the excited dienol-to-monoketo tautomer (<100 fs), followed by the monoketo-to-diketo step (with a time constant of a few ps). The proton-transfer dynamics has been studied in the sol−gels TMSPM and TMOS, both as a function of the temperature and as a function of the wavelength of the excitation pump pulses. In the sol−gel TMSPM, the proton-transfer dynamics in photoexcited $BP(OH)_2$ is faster than the dynamics of the solute in TMOS and also faster than that in liquid solution (as known from our previous work). In the sol−gel TMOS, which contains residual amounts of methanol and water, the proton-transfer dynamics is found to be influenced by the solvation of the $BP(OH)_2$ solute to the nearby layers of methanol and water. In the two-step process, the ratio of the yields of the monoketo and diketo tautomers is significantly reduced when excitation is to lower excited-state energies. It is discussed that this effect is typical of an energy barrier in the dienol-to-monoketo reaction pathway, the barrier height being more pronounced in the TMSPM glass than in the case of the TMOS glass ($\sim$300 cm^{-1}). At higher excitation energies, the results for the ratio of the yields of the monoketo and diketo tautomers are suggestive of additional dark processes due to coupling to the rigid sol−gel network.

1. Introduction

In recent years, several experimental and theoretical studies of ultrafast excited-state intramolecular proton-transfer (ESIPT) reactions have been reported.[1−21] In the experiments, ultrashort laser pulses are applied to excite the protic molecules to an electronic state in which the electronic charge distribution is quite different from that in the ground state, and thus, the corresponding excited-state and ground-state potential energy surfaces, as a function of the normal mode coordinates, are also appreciably different.[3] Since the nuclear motions cannot adiabatically follow the laser-induced sudden changes in the electronic charge distribution, the impulsive photoexcitation prepares the molecule in a nonstationary state, and a molecular relaxation over the excited-state potential energy surface ensues until the new equilibrium positions for the nuclei are obtained. When the vibrational modes active in the relaxation process involve large amplitude proton motions as, for example, in hydrogen-bridge formation, then the amplitude of these proton displacements is often large enough that the proton transfer can be considered separately.[3,5] The usual time scale for such proton-transfer processes extends from tens of femtoseconds to picoseconds. Single (see, e.g., refs 7−11) and double (see, e.g., refs 2, 5, and 6) ESIPT dynamics have been studied.

For [2,2′-bipyridyl]-3,3′-diol (henceforth referred to as $BP(OH)_2$), it was previously shown[22−24] that the optical absorption and fluorescence band maxima are practically independent of the polarity of the solvent. Supported also by the results of their semiempirical calculations, Bulska et al.[22,23] concluded that photoexcitation of the molecule is from the dienol ground-state to the excited-state dienol configuration, followed by a cooperative double proton-transfer process in the excited state, thus forming the fluorescent diketo tautomer. Kaschke et al.[25] performed a picosecond study of $BP(OH)_2$ (with a time resolution of about 5 ps). They found that the initially excited S_1 state decays in a few picoseconds. This time was considered as being characteristic for the double proton-transfer process. Evidence for a stepwise dual proton transfer was not found although INDO calculations predicted that the excited singlet state of the monoketo tautomeric form is between that for the first excited states of the dienol and diketo forms.[22]

Utilizing fluorescence up-conversion techniques, we recently reported studies of the ESIPT dynamics in $BP(OH)_2$ on a femtosecond time scale.[6] It was shown that the dual proton transfer in photoexcited $BP(OH)_2$, in liquid solution, can take place in either of two ways, a concerted one-step process yielding directly the diketo product or a sequential two-step process, in which first the monoketo intermediate is formed and then the diketo product in the second step. The concerted reaction and the first step in the sequential process were too fast to be resolved in the experiment (<100 fs); the mono-to-diketo reaction in the two-step mechanism occurred with a typical time constant of 10 ps. Intramolecular stretching and bending modes were considered to promote the one-step and

† Permanent address: Department of Physics and Instituto Nazionale di Fisica della Materia, University of Rome "Tor Vergata", Via della Ricerca Scientifica, 1, 00133 Rome, Italy.

10.1021/jp981830q CCC: $15.00
Published on Web 10/13/1998

two-step double proton-transfer reactions, respectively.[2] In aprotic solvents, the ESIPT dynamics appeared insensitive to the polarity and viscosity of the solvent. In protic solvents, on the other hand, the proton transfer in the mono-to-diketo reaction slowed down as the solvent viscosity was increased. It was conjectured that the "free" nitrogen atom in the pyridyl ring of the monoketo tautomer intermediate could form a hydrogen bridge to a neighboring protic solvent molecule, the lifetime of this protonated intermediate being on the order of the solvent rotational diffusion time.

It has been considered that $BP(OH)_2$ is a suitable laser dye material.[26] In fact, laser activity has been demonstrated for $BP(OH)_2$ dissolved in different solvents (benzene, dioxane, cyclohexane, etc.[26]). In view of this, optical studies of $BP(OH)_2$ dissolved in sol−gel glass matrixes have been performed.[27] Silica glasses obtained through sol−gel synthesis have received considerable attention in recent years because of their wide application in integrated optics.[28−33] The incorporation of organic molecules in sol−gel hosts, thanks to low preparation temperatures, has the great advantage of combining the particular optical properties of the organic compounds, such as high photoluminescence efficiency with the low optical losses, long-term stability, and mechanical workability of glasses.[34−38]

The optical properties of molecules may be severely modified when dissolved in glassy matrixes as compared to those in liquid solution.[27,34,39−44] An example of this is $BP(OH)_2$.[27] To further study the ESIPT of the $BP(OH)_2$ system, when dissolved in inorganic and hybrid sol−gel silica glass matrixes, we have performed femtosecond fluorescence up-conversion experiments. Very recently, the first ultrafast studies of excited-state intramolecular proton transfer in confined systems were reported.[10] In this paper, we report results of similar investigations for $BP(OH)_2$ in two different sol−gel matrixes, to establish the role of rigidity and polarity of the solid matrixes on the proton-transfer dynamics. One of the sol−gel matrixes is a plain sol−gel (TMOS, cf. Experimental Section) obtained by slow hydrolysis and polycondensation of tetramethyl orthosilicate; the second sol−gel (TMSPM, cf. Experimental Section) is a hybrid system in which an organofunctional alkoxysilane has been added.[27,45,46] We find, as before in the liquid phase,[6] that in the sol−gel solid two competitive intramolecular proton-transfer pathways occur, a concerted single-step double proton transfer (in less than 100 fs) and, parallel to this, a stepwise double proton transfer where the monoketo intermediate is formed instantaneously and decays into the diketo excited tautomer in about 5 ps. Moreover, we present results of our study of the influence of the amount of excited-state vibronic excess energy on the relative yield of the monoketo and diketo excited-state photoproducts of $BP(OH)_2$. We show that the amount of excess vibrational energy significantly influences this ratio and, in fact, gives rise to photoselectivity in the proton-transfer mechanism which reveals itself only because of the high-time resolution of the experiments. The outline of the paper is as follows. In the Experimental Section, experimental details are presented. In Section 3, we present the experimental results, i.e., those obtained by means of steady-state spectroscopy, the results of the time-resolved fluorescence measurements with femtosecond and picosecond time resolution, and the effects of the excitation wavelength on the temporal behavior (in the subpicosecond time regime) of the fluorescence of $BP(OH)_2$ in sol−gel material. Finally, in Section 4, the experimental data are discussed in relation to the mechanisms and dynamics of the double proton-transfer processes in the excited state of $BP(OH)_2$ in sol−gel material.

2. Experimental Section

$BP(OH)_2$ was purchased from Aldrich and used without further purification. Bulk sol−gel glasses were prepared using tetramethyl orthosilicate (TMOS) as a precursor and formamide as a drying control chemical additive.[47,48] Molar ratios of the reagents were TMOS:water:formamide:methanol = 1:10:2:7. Sol−gel glasses modified by organic side groups were prepared using 3-(trimethoxysilyl)-propyl methacrylate (TMSPM) and tetramethyl orthosilicate as precursors.[27] In these samples an organic network in addition to the inorganic one is formed.[45,46] Molar ratios of the components were TMSPM:TMOS:water = 1:1:3.5. In the following, we indicate the samples described above as TMOS and TMSPM, respectively. The $BP(OH)_2$ dye was dissolved in the sol liquid solution with an approximate initial concentration of 1.3×10^{-4} M and 3.5×10^{-4} M for the TMSPM and TMOS sol−gel glasses, respectively. Immediately after preparation, the samples were stored in an oven at about 38 °C. After the samples were aged for a period of about three weeks, we obtained sol−gel glasses (thickness 2−3 mm) ready to be used in the experiments.

Steady-state absorption spectra were recorded by means of a conventional spectrophotometer (Shimadzu UV-240). The steady-state fluorescence spectra were measured using the emission spectrometer described before.[49] The emission spectra were corrected for the wavelength-dependent sensitivity of the monochromator-photomultiplier detection system.

Femtosecond and picosecond fluorescence transients were measured by means of two different experimental setups. Femtosecond laser excitation was accomplished using a diode-pumped continuous wave (cw) Millennia X Nd:YVO_4 laser which pumped a Tsunami Ti:sapphire laser operating at 800 nm and which delivered 60 fs pulses at a repetition rate of 82 MHz. The laser pulses were first amplified in a Quantronix regenerative amplifier laser system to about 400 mW at 1 kHz and then split into two beams by a beam splitter. One of the beams was led into an OPA system. The fourth harmonic (less than 0.1 μJ and 100 fs) was selected by a 2-mm thick optical filter DUG 11 (from 300 to 400 nm) and attenuated by an optical filter. It was used to photoexcite the sample which was moving back and forth perpendicular to the excitation laser beam to avoid the heating of the sample. The ensuing transient fluorescence was time-resolved detected, applying the fluorescence up-conversion detection technique.[50−52] In the latter experiments, an attenuated part of the fundamental beam (800 nm) was led through a delay line and focused, together with the pump-pulse induced fluorescence, onto a 1-mm thick BBO crystal (type I phase matching condition). The up-conversion signal (at the sum frequency of the fluorescence and the fundamental of the fs laser) was filtered out by an UG 11 filter and then focused on the entrance slit of a Zeiss M 20 monochromator and photodetected by means of a photomultiplier (EMI 9863 QB/350) connected to a SRS lock-in amplifier system linked to a personal computer for data storage and analysis. To avoid detection of kinetics due to reorientational motions of the probed $BP(OH)_2$ molecules, the polarization of the excitation beam was at the magic angle of 54° 44′ with respect to the vertically polarized gating beam. From the measured cross-correlation function of the excitation and gating pulses at 400 and 800 nm, the instrumental time response was estimated to be approximately 300 fs (fwhm).

Fluorescence transient measurements with picosecond time resolution were conducted using the time-correlated single-photon counting technique.[49] Briefly, a mode-locked Coherent Innova 200-15 Ar^+ ion laser synchronously pumped a Coherent

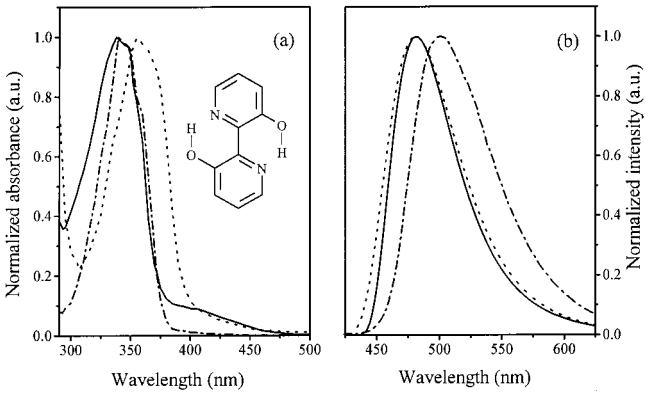

Figure 1. Steady-state absorption (a) and emission (b) spectra of BP-$(OH)_2$ in TMOS sol−gel glass (solid curves), in TMSPM sol−gel glass (dotted curves), and in cyclohexane solution (dashed−dotted curves) at room temperature. A schematic picture of the structure of the dienol form of $BP(OH)_2$ has been inserted in (a).

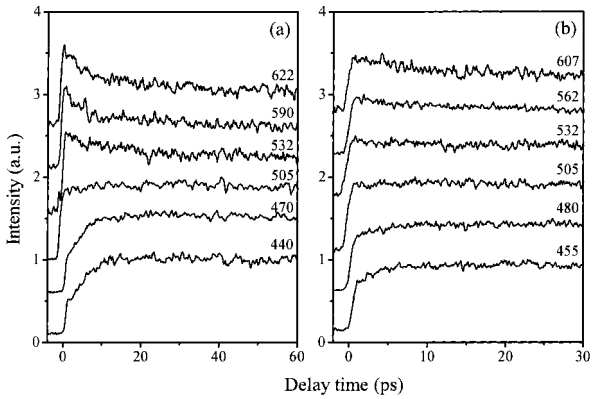

Figure 2. Fluorescence up-conversion transients of $BP(OH)_2$ in (a) TMOS and (b) TMSPM sol−gel glasses for various detection wavelengths at room temperature. Excitation pulse is at 320 nm. The detection wavelengths are shown in nm.

702-3 dye laser with a Coherent 7200 cavity dumper. The cavity-dumped dye laser generated laser pulses of about 7 ps (fwhm autocorrelation trace) and 25 nJ at 3.7 MHz. These pulses were then frequency doubled to about 320 nm in a 6-mm BBO crystal and used to photoexcite the sample. The fluorescence transients were detected, applying the time-correlated single-photon counting technique in reverse mode. The output of the photomultiplier, amplified using a Hewlett-Packard 8347A 3 GHz amplifier, was sent to a (modified) Tennelec 455 constant fraction discriminator, and finally it acted as the start pulse for the Tennelec TC 864 time-to-amplitude converter. Part of the 644-nm dye laser pulse was monitored by an Antel FS 1010 photodiode. This photodiode signal was then sent to a Tennelec TC 454 constant fraction discriminator as the stop pulse. The output of the TC 864 was fed into an EG&G Ortec 918 multichannel buffer. The time-base of the TC 864 was calibrated to an accuracy of 1% by optically delaying the arrival of the visible dye laser pulse at the photodiode with respect to the arrival of the UV excitation pulse at the sample. The instrument response was about 16 ps (fwhm). All of the fluorescence transients were measured at magic angle.

3. Results

(a) Steady-State Spectroscopy. The steady-state absorption and emission spectra for $BP(OH)_2$ in TMOS and TMSPM sol−gel glasses are given in Figure 1. Absorption and emission spectra for $BP(OH)_2$ dissolved in cyclohexane are also presented in the same figure for comparison (from ref 6). The band maxima in the absorption spectra for $BP(OH)_2$ in TMOS and cyclohexane are found to coincide near 340 nm, whereas the band maximum for the TMSPM sample is shifted to about 360 nm. In the emission spectra, band maxima for the TMOS and TMSPM samples coincide at approximately 480 nm, whereas that for the cyclohexane solution is red-shifted (by about 1200 cm^{-1}). The steady-state absorption and emission spectra for $BP(OH)_2$ in the sol−gel glasses are in good agreement with those reported previously by Eyal et al.[27]

(b) Femtosecond Up-Conversion Experiments. Figure 2 shows some typical fluorescence transients for $BP(OH)_2$ in TMOS and in TMSPM hosts at different detection wavelengths (in the range 440−620 nm) for a fixed excitation wavelength of 320 nm of the pulses delivered by the OPA laser system and using time windows of about 66 and 33 ps, respectively. The time-resolved fluorescence transients show a very fast (instantaneous) rise within the duration time of the laser pulses. This was made more clear in experiments where the shortest time window, with a span of 6.7 ps, was used. The instantaneous rise component is followed by an additional rise, when detection is at wavelengths below 520 nm, or a decrease, at detection wavelengths above 520 nm, on a picosecond time scale. Finally, the fluorescence decays slowly with a time constant of several nanoseconds, typical of the lifetime of the fluorescent state. This slow decay component is not resolved in the transients of Figure 2 but was clear when repeating the experiments for longer delay times using the picosecond fluorescence setup outfitted with time-correlated single photon counting detection equipment.

The fluorescence transients observed for $BP(OH)_2$ doped in the sol−gel matrixes are very similar to those measured for the same solute in various liquid solvents. As before,[6] the measured transients could be fitted to a biexponential function of the form of eq 1, convoluted with the system response function. For

$$I(\lambda, t) = c_1(\lambda)\{\exp(-t/\tau_2) - \exp(-t/\tau_1)\} + c_2(\lambda)\exp(-t/\tau_2) \quad (1)$$

the transients detected on the blue side of the emission ($\lambda <$ 520 nm), after the sharp rise, the intensity rise of the $BP(OH)_2$ fluorescence transients could be fitted with a time constant (τ_1) of about 5 ps for the TMOS sample and of about 3 ps for the TMSPM sample. The picosecond intensity decrease component, when detection is at the red part ($\lambda >$ 520 nm), could be fitted with the same time constants, i.e., 5 ps for the TMOS sample and 3 ps for the TMSPM sol−gel glass. The slow lifetime component (τ_2) fitted a second exponential term with decay times of 1.8 ns and 4.8 ns for the TMOS and TMSPM samples, respectively.

The wavelength dependence of the (sub)picosecond fluorescence transients of $BP(OH)_2$ is very similar to that previously reported for $BP(OH)_2$ in liquid solution.[6] In the latter case, on the basis of the time dependence of the fluorescence spectrum as reconstructed from the measured fluorescence transients, it was discussed that intramolecular single and double proton-transfer processes occur in $BP(OH)_2$ in the excited state. Likewise, we have measured fluorescence transients for BP-$(OH)_2$ in the sol−gel glasses, as in Figure 2, in the detection wavelength range from 440 nm up to 620 nm, with 10-nm intervals. We used these data to reconstruct the fluorescence spectra for $BP(OH)_2$ in both sol−gel glasses, at different delay times, following the spectral reconstruction method described by Maroncelli and Fleming.[53] Briefly, as mentioned above, the experimental transients were fitted to a biexponential function of the form of eq 1, convoluted with the system response

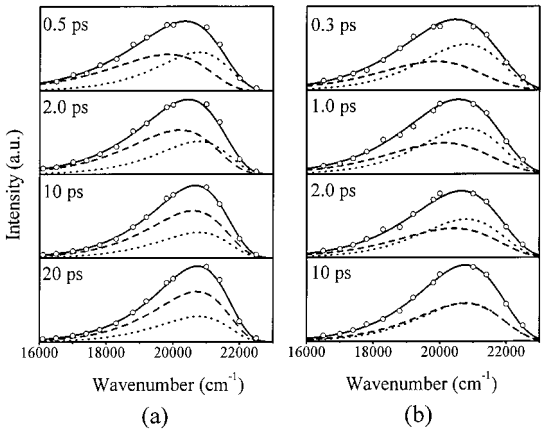

Figure 3. Time-resolved reconstructed emission spectra of $BP(OH)_2$ in (a) TMOS and (b) TMSPM sol−gel samples at room temperature. Solid curves are the total emission spectra. Dotted curves are the emission spectra of the diketo tautomer component formed instantaneously from the dienol tautomer. Dashed curves represent the difference between the total emission spectra and the instantaneously formed diketo emission spectra. The delay times in ps are indicated in the panels. Open circles represent data points obtained in the spectral reconstruction procedure and used for the log-normal fittings of the spectra.

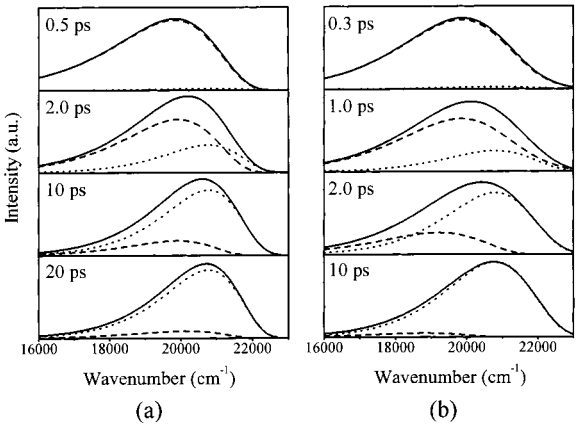

Figure 4. Decomposition of the difference emission spectra (full curves) of $BP(OH)_2$ into the monoketo and diketo emission spectra in (a) TMOS and (b) TMSPM sol−gel samples at room temperature. The full curves are identical to the difference spectra (dashed curves) of Figure 3. Dashed curves represent the emission spectra of the intermediate monoketo tautomer. Dotted curves represent the emission spectra of the diketo tautomer formed from dienol via the monoketo tautomer.

function. After being corrected for the wavelength dependence of the detection sensitivity, the spectrum at some delay time could be reconstructed point-by-point using the calibrated fits to the transients, obtained at the series of detection wavelengths. To smooth the spectrum, the point-by-point spectrum was fitted to a log-normal shape function. The band spectra in Figure 3 (cf. drawn lines in the figure) are illustrative of the thus-obtained spectra of $BP(OH)_2$ in the TMOS (Figure 3a) and TMSPM (Figure 3b) sol−gel samples, at different delay times.

The high-energy part of the time-resolved emission band spectra, measured immediately after the pulsed excitation, appears to coincide with that known for the steady-state emission of the diketo tautomer in liquid solution.[23,26] We consider this to be evidence that, at least in part, the observed emission is due to the diketo tautomer. We thus assume now, as was done before,[6] that the reconstructed time-resolved emission spectrum can be considered as a superposition of two parts, one component which is representative of an instantaneously formed diketo tautomer emission (and which decays in several ns) and the other component being a new, hitherto not observed part which is the difference spectrum (dashed lines in Figure 3) of the reconstructed spectrum (full lines in Figure 3) and the extrapolated diketo spectral contribution (dotted lines in Figure 3). The difference spectrum has a typical dynamic shift of several ps, whereas the instantaneously formed diketo component decays only slightly on the picosecond time scale, in accordance with its lifetime of a few ns. The difference (dashed) component clearly exhibits a blue shift as time progresses.

Since, for increased delay times, the difference spectrum and the diketo spectrum become more alike, we propose (see also Discussion) that the difference spectrum initially is due to a precursor species which decays into the diketo excited state as time progresses. Eventually, only the emission of the diketo tautomer survives, that is, for times longer than about 20 ps after the pulsed excitation. As discussed in Section 4, we attribute the short-living new emission, that precedes the diketo emission, to the emissive monoketo tautomer precursor of the diketo tautomer. To obtain the emission spectrum characteristic of this short-living monoketo tautomer, we have decomposed the newly found spectra (dashed curves of Figure 3) into a diketo spectral contribution and a short-living new spectrum, which is considered to be representative of the fluorescence spectrum of the monoketo tautomer. The short-lived spectra thus obtained and their time dependences are illustrated by the spectra of Figure 4. In this figure, the dashed spectra are representative of the monoketo precursor to the diketo spectral product, the dotted spectra are representative of the diketo product formed from the monoketo precursor, whereas the full lines are identical to the difference spectra of Figure 3. It is found that the spectrum attributed to the monoketo intermediate has an emission band maximum at 505 nm. Furthermore, the monoketo emission decays monoexponentially with a typical time constant of 5 ps for $BP(OH)_2$ in TMOS and a somewhat shorter decay of 3 ps, when the solute is in TMSPM. For both samples, concomitant with the monoketo emission decay, a rise of the diketo emission is observed with the same time constant. The picosecond decay of the monoketo component and the concomitant rise of the diketo component effectively result in the time-dependent blue shift illustrated in Figure 3. In summary, the spectral analysis of the femtosecond fluorescence upconversion transients for $BP(OH)_2$ in sol−gel glasses yields two spectral components that are formed instantaneously (<100 fs); one (with a band maximum at 505 nm) is attributed to the monoketo intermediate, and the second (with its band maximum at 480 nm) is representative of the diketo tautomer emission. The monoketo intermediate has a lifetime of a few picoseconds and decays into the diketo tautomer.

(c) Temperature Dependence of Transients. The fluorescence transients measured for both sol−gel samples with the picosecond setup were also investigated as a function of the temperature. In these experiments, the excitation wavelength was 322 nm, the detection was at 460 nm, and the fluorescence was followed using a time window of about 5 ns after the excitation pulse. Typical results are given in Figure 5. From Figure 5a (for TMOS), it is seen that, as the temperature is lowered, the picosecond rise component that is after the instantaneous component and that is characteristic of the monoketo-to-diketo conversion, slows down. Moreover, we find a longer lifetime for the emissive state of the diketo tautomer. The measured transients convoluted with the response function were fitted to eq 1, where τ_1 is the time constant of the mono-to-diketo reaction and τ_2 is the lifetime of the emissive diketo

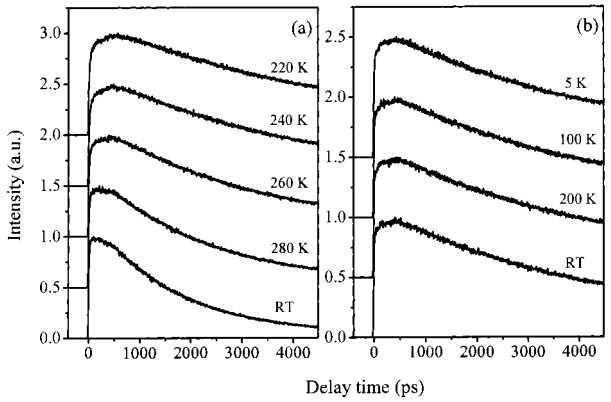

Figure 5. Picosecond fluorescence transients of $BP(OH)_2$ in (a) TMOS and (b) TMSPM sol−gel glasses at various temperatures. Excitation wavelength is 322 nm, and detection wavelength is 460 nm. The temperatures are as indicated in the figure.

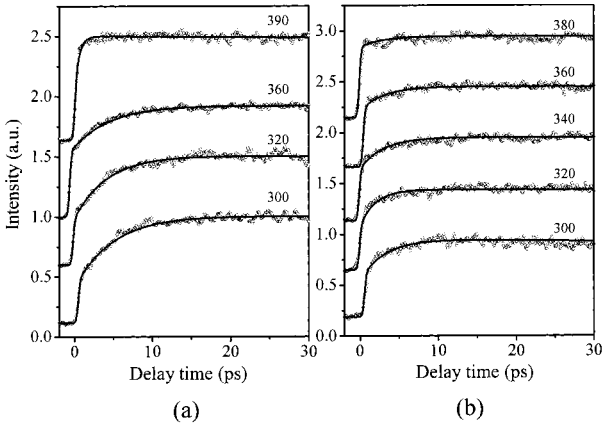

Figure 6. Femtosecond fluorescence transients of $BP(OH)_2$ in (a) TMOS and (b) TMSPM sol−gel matrixes for various excitation wavelengths, at room temperature. The excitation wavelengths are indicated in nm in the figure. The emission is detected at 460 nm. The solid curves represent the best fits with the biexponential function given in eq 1 to the experimental points.

tautomer. For $BP(OH)_2$ in the TMOS glass (Figure 5a), the time constant of the rise component increases from 5 ps to about 300 ps, when the temperature is decreased from room temperature to about 220 K. In the same temperature range, the lifetime of the diketo tautomer changes from 1.8 ns at room temperature to about 5.0 ns at 220 K. Below 220 K, the initial transparency of the TMOS sol−gel glass disappeared, and the sample became opaque. For TMOS samples that have aged for a few weeks, it is known that the pores of the sol−gel glass contain residual amounts of solvent (basically water and methanol).[41,47,48] The observed opaqueness at the lower temperatures may result from the freezing and cracking of the solvent residues in the sol−gel. No solvent residues are present in the TMSPM sol−gel glass. This explains why the fluorescence transients for $BP(OH)_2$ in the TMSPM glass (Figure 5b) could be followed down to 5 K. No temperature dependence was detected from room temperature down to 5 K, neither for the fast rise time component (3 ps) nor for the long lifetime component (4.8 ns).

(d) Excitation Wavelength Dependence of Fluorescence Transients. Very recently, we reported a switch of the ESIPT mechanism in $BP(OH)_2$, in liquid solution, when the excitation wavelength was chosen to be 380 nm instead of 267 nm.[4] At the lower excitation energies, it appeared that the two-step process was suppressed, and when ultimately the excitation was at 380 nm, the yield of the stepwise double proton transfer was reduced to about 10% of its original value. We have now repeated these experiments for $BP(OH)_2$ in TMOS and TMSPM sol−gel glasses. Using the OPA laser system, the excitation wavelength in the fluorescence up-conversion experiments was varied from 300 to 390 nm. The fluorescence up-conversion measurements were performed with the detection wavelength maintained at 460 nm. At this wavelength, the emission is almost exclusively due to the diketo tautomer. Figure 6 shows a few typical time-resolved fluorescence up-conversion transients for the TMOS and TMSPM samples. All transients show an immediate rise (within the response time of the laser pulse) due to the instantaneously produced diketo tautomeric product. The immediate rise is followed by a slower component due to the conversion of the also instantaneously produced monoketo tautomer intermediate into the diketo form, with a time constant of the order of a few picoseconds. A remarkable feature occurs when the excitation wavelength is changed from 300 nm up to 390 nm; the relative amplitudes of the two fluorescence components, that is, the instantaneously formed and the picosecond rise components are is drastically affected. In particular, the ratio of the amplitudes of the instantaneous and the rise components increases as the excitation energy is lowered. As mentioned above, the instantaneous component is attributed to the instantaneously formed diketo tautomer, and the rise component is due to the decay of the intermediately formed monoketo tautomer into the diketo form. Thus, the change in the ratio of the amplitudes as the excitation energy is lowered implies that the formation of the monoketo component is suppressed, or in other words, in the initial ultrafast decay of the excited dienol form (<100 fs) resulting in the formation of the monoketo and diketo tautomers, the diketo becomes favored.

4. Discussion

The fluorescence transients of Figure 2 are very similar to those observed for $BP(OH)_2$ in liquid solution. The picosecond decay when detection is on the red side of the emission band and the picosecond rise in the blue part of the emission exclude a dynamic Stokes shift as the explanation for this variation of the transients with the detection wavelength. On the contrary, as discussed in Section 3c, the phenomena are compatible with the occurrence of a short-lived new emission band, peaking at 505 nm, with a lifetime of 5 ps for $BP(OH)_2$ in the TMOS sample and 3 ps for the fluorescent solute in the TMSPM sol−gel glass. Since the "new" transient emission band, with its maximum at 505 nm, decays into the eventual diketo emission (equal decay and rise times, respectively), it is most likely that this emission band originates in a species that is a precursor of the diketo tautomer. We propose that the emission is characteristic of the monoketo tautomer form of $BP(OH)_2$ in sol−gel glasses. Alternatively, one might consider the possibility that the precursor state of the diketo emission is the dienol state and that therefore the 505-nm emission would correspond to the normal fluorescence of $BP(OH)_2$ in its dienol form. However, this would imply, on one hand, that the dienol excited state would have a lifetime of several picoseconds since in the stepwise reaction path the precursor state decays in a few picoseconds (vide supra), and on the other hand, it follows from the time-resolved experiments that the diketo form could be formed instantaneously and that therefore the same dienol state should decay within 100 fs. Obviously, the latter lifetime is inconsistent with the aforementioned lifetime of a few picoseconds. Thus, to explain the occurrence of both an instantaneously formed diketo component and a diketo component

TABLE 1: Emission Band Maxima of the Monoketo (λ_{MK}) and Diketo (λ_{DK}) Tautomers of $BP(OH)_2$ Dissolved in Cyclohexane and in TMOS and TMSPM Sol−Gel Glasses at Room Temperature[a]

	cyclohexane	TMOS	TMSPM
λ_{MK} (nm)	568	505	505
λ_{DK} (nm)	510	480	480
τ_1 (ps)	10	5	3
τ_2 (ns)	3.0	1.8	4.8

[a] The corresponding time constants of the mono-to-diketo reaction (τ_1) and the lifetimes of the diketo tautomer (τ_2) are also presented.

formed on a picosecond time scale, one needs to invoke a short-lived intermediate state, with a lifetime of a few picoseconds, which could provide for a second reaction pathway to produce the diketo form. The most likely candidate for this precursor of the diketo form is, of course, the monoketo tautomer excited state. This state was predicted in semiempirical calculations to have its energy between that of the excited dienol and diketo states.[22] Moreover, we note that the position of the emission band maximum in the liquid almost coincides with that of the BPOH molecule which, of course, is capable of only a single proton transfer in its excited state.[23] We conclude that (i) the spectroscopic results for $BP(OH)_2$ in sol−gel glasses are quite similar to those for the same solute in liquid solution and that (ii) in particular from the excited-state dynamics results, the simultaneous presence of one-step and two-step processes can explain the double proton transfer.

As summarized in Table 1, the positions of the maxima of the emission bands characteristic of the monoketo and diketo tautomers, in both sol−gel samples, are blue-shifted with respect to the corresponding bands for $BP(OH)_2$ dissolved in cyclohexane. The results are suggestive of the weaker molecular force fields exerted by the sol−gel surroundings on the $BP(OH)_2$ solute as compared to the situation of liquid solution.[34,39] For example, in the TMOS sol−gel glass, the average pore size is about 26 Å in diameter[39] and probably even smaller for TMSPM where the pores are partially filled by the organic network. It is likely that, because of the small size of the pores, the $BP(OH)_2$ molecules in sol−gel are surrounded by only a few layers of protic solvent molecules. This may be of influence on the total solvent shift of the solute molecular energies. In addition, McKiernan et al.[41] demonstrated that a consistent blue shift of the emission band occurs as the rigidity of the matrix increases. Casalboni et al.[39] observed a blue shift of the emission band and an increased photoluminescence lifetime as the average pore size decreases. We suggest that the rigidity may also affect the difference between liquid and sol−gel systems.

The blue shift of the emission band in the sol−gel with respect to the liquid solution is about 2200 cm^{-1} for the monoketo and 1200 cm^{-1} for the diketo. It is likely that, in liquid solution, the monoketo tautomer is more stabilized with respect to the diketo tautomer because of its larger dipole moment.[23] From the different stabilization of the two excited tautomers, it may also be that the energy barrier separating the monoketo excited-state minimum energy from the more stable diketo excited-state energy minimum is less in the sol−gel than in the liquid solution. This may account for the faster monoketo-to-diketo conversion in the sol−gel host (5 ps versus 10 ps). The lifetime of the diketo excited state may also be affected by the rigidity of the cage which reduces the effectiveness of nonradiative decay.[34,36,39] This is compatible with the longer lifetime of 4.8 ns in TMSPM, as compared to 3.0 ns in cyclohexane. For TMOS sol−gel glasses, the pores still contain

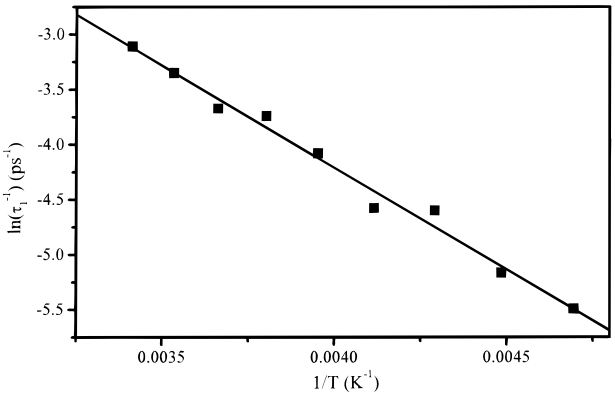

Figure 7. Temperature dependence of the mono- to-diketo reaction rate of $BP(OH)_2$ in TMOS sol−gel glass. The squares are the experimental points. The solid line represents the best linear fit.

protic solvent molecules, even after a few weeks of aging.[47,48] Inside the TMOS pores, the $BP(OH)_2$ molecule may therefore still contain one or a few solvation layers, and therefore, the lifetime of 1.8 ns of the diketo state in TMOS should be compared with that of 1.0 ns[27] for the solute in water solution or 1.2 ns in methanol solution as measured.

As illustrated by the transients in Figure 5, upon the sample being cooled, the picosecond rise component slows down for the TMOS sample, but no such behavior is found for the TMSPM sample. In view of the discussion given above, the temperature dependence of the fluorescence transients for the TMOS sample shows that in this case the rate of the monoketo-to-diketo reaction step is temperature dependent, whereas this temperature dependence is absent in the TMSPM sample. Very recently, we reported on the influence of the solvent layers surrounding the $BP(OH)_2$ molecules on the proton-transfer dynamics in liquid solution.[2] In aprotic solvents, the proton transfer dynamics remained unaffected when the solvent polarity or the viscosity was changed. By contrast, in protic solvents the reaction rate constant decreased as the viscosity increased. As mentioned above, in TMSPM, the pore network is mainly filled by the propyl methacrylate groups,[27,38,45] but for TMOS sol−gel glasses, it is known that the pores contain small amounts of protic solvent molecules[41,47,48] and the cage may be regarded as a hydroxylic environment for the silanol groups.[34,44] It is likely, therefore, that the temperature effect on the proton-transfer dynamics in the TMOS sample can be attributed to the influence of the protic molecules surrounding the $BP(OH)_2$ molecules. Apparently, the solvating protic molecules in the TMOS glass still have motional freedom, and this, in fact, may not be significantly different from that in the bulk liquid. This is also borne out by the temperature dependence of the decay time τ_1. In Figure 7 we present an Arrhenius plot for τ_1. A linear dependence is obtained, and the extrapolated activation energy is 15.4 kJ/mol. This value is somewhat larger than that for the activation energies found for the monoketo-to-diketo conversion for $BP(OH)_2$ dissolved in methanol, ethanol, or propanol.[2] For the latter, the activation energies were found to correspond to the activation energies of the viscosity coefficient of the solvent. Possibly, the higher activation energy found in the sol−gel glasses is indicative of a stronger sticking within the solvent layers in the sol−gel pores as compared to the situation in the liquid. This increased "viscosity" may reflect the influence of the pore size on the solvent mobility.

As is evident from the transients shown in Figure 6, for higher excitation wavelengths, the amplitude of the instantaneous component in the diketo emission is enhanced as compared to

the amplitude of the picosecond component. From the relative suppression of the diketo product formed from the monoketo intermediate, when applying lower excitation energies, it follows that under these excitation conditions the amount of monoketo tautomer has become less and hence also the amount of diketo that can be obtained from it. Thus, the amplitudes of the transients shown in Figure 6 can be considered as a measure of the relative yield of the instantaneously formed monoketo and the instantaneously formed component of the diketo tautomer, respectively. The decrease in the yield of monoketo intermediate when lowering the excitation energy obviously implies that in the trajectory for the dienol-to-monoketo reaction the system passes an energy barrier.

At all excitation wavelengths, as before, the fluorescence transients could be fitted to the biexponential function of eq 1. In the excitation wavelength range 300−390 nm, the short-time rise component, τ_1, was always found to be 5 ps for TMOS and 3 ps for TMSPM, and for the long-time decay component, τ_2, values of 1.8 and 4.8 ns were obtained for the TMOS and TMSPM samples, respectively. The drawn curves in Figure 6 are illustrative of the best-fit results using eq 1. The proportionality constants, $c_1(\lambda)$ and $c_2(\lambda)$, are found to vary significantly with the excitation wavelength. In Figure 8, we plot the ratio, c_1/c_2, as deduced from the fittings for the applied excitation wavelengths, for the TMOS and TMSPM samples. Evidently, as the excitation energy is lowered, the magnitude of the c_1/c_2 ratio becomes smaller until for an excitation energy of 25 600 cm^{-1} virtually no monoketo can be resolved to decay into the diketo tautomer. As mentioned, this is evidence for the existence of an energy barrier in the first step of the two-step reaction pathway, that is, the dienol-to-monoketo conversion. Very recently, a similar phenomenon has been reported for $BP(OH)_2$ in liquid solution.[4]

To estimate the height of the energy barrier in the aforementioned first step, we apply a simplified model in which we assume tunneling through the barrier to be the main process involved in the dienol-to-monoketo conversion. We consider a parabolically shaped barrier of the form

$$V = V_0 - {}^1/_2 Ax^2 \qquad (2)$$

where V_0 is the maximum potential energy, $A > 0$, and x is representative of the tunneling coordinate. Following ref 54, the expression for the permeability, G, becomes

$$G = \{1 + \exp[2\pi m^{1/2}(V_0 - W)/\hbar A^{1/2}]\}^{-1} \qquad (3)$$

where G is the ratio between the fluxes of the transmitted and incident tunneling particle, that is, $G = (k_T/k_I)|A_T|^2$, where k_T/k_I is the ratio of the velocities of the transmitted and incident particle and $|A_T|^2$ represents the particle density of the transmitted particle, W is the excitation energy. The plot of a best fit function, in accordance with eq 3, to the experimentally determined values of c_1/c_2 versus the excitation energy, is included in Figure 8. The values of the parameters for the plotted curves of Figure 8 are $V_0 = 27\,700$ cm^{-1} and $A/m = 1.5 \times 10^{30}$ s^{-2} for TMOS and $V_0 = 28\,000$ cm^{-1} and $A/m = 4.3 \times 10^{30}$ s^{-2} for TMSPM.

The 0−0 electronic transition for $BP(OH)_2$ is estimated to be at 27 400 cm^{-1} in liquid solution.[55] Since the absorption band of $BP(OH)_2$ in TMOS is not shifted with respect to the absorption in cyclohexane (cf. Figure 1a), it is likely that the 0−0 transition in TMOS is at the same energy as in the liquid solution. Taking the value for W as 27 400 cm^{-1} and the fitted value of 27 700 cm^{-1} for V_0 in TMOS, it follows that the barrier

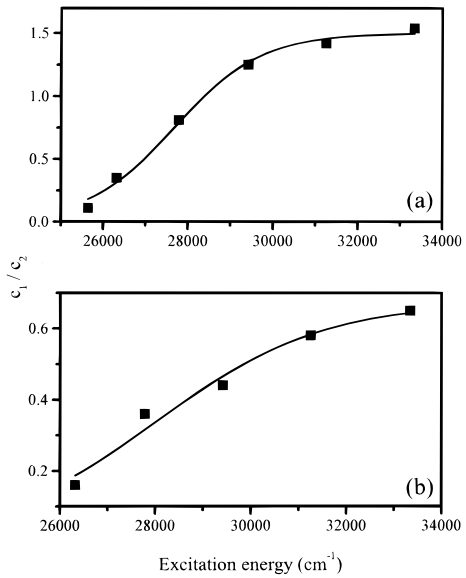

Figure 8. Ratio of the yields of the instantaneously formed monoketo (c_1) and diketo (c_2) tautomers for $BP(OH)_2$ in (a) TMOS and (b) TMSPM sol−gel glasses. The squares represent the ratio as obtained from the measured fluorescence transients. The solid curves represent the best fit curves according to eq 3.

height, according to the simplified model, is approximately 300 cm^{-1}. For $BP(OH)_2$, in apolar liquid solution, we have similarly found previously[4] a barrier height of 600 cm^{-1}. Thus, considering the crudeness of the model, we estimate somewhat lower barrier heights when comparing the activation energies for the dienol−monoketo conversion step in the sol−gel with that in apolar liquid solution.

We remark that in aprotic liquid solution a tunneling mechanism for the monoketo-to-diketo proton-transfer step was previously excluded on the basis of the lack of an isotope effect in the excited-state dynamics.[2] In protic solvents, on the other hand, deuteration of the solvent hydroxyl groups produced a slowing down of the monoketo-to-diketo proton-transfer dynamics; however, this effect turned out to be caused by the change of the viscosity of the solvent, and no indication for a proton-tunneling mechanism was found. Since deuteration did not directly affect the proton-transfer dynamics, it was concluded that in $BP(OH)_2$ the proton-transfer results from vibrational mode motions for which the effective mass is determined by many moving nuclei in the molecule and not just by the hydroxyl protons. On the basis of the almost identical excited-state dynamic behavior of $BP(OH)_2$ in liquids and sol−gel glasses, it is very likely that also in sol−gel glasses the intramolecular proton transfer is assisted by vibrational stretching (for the concerted process) and bending (for the two-step process) modes. A scheme summarizing some of the details in the proton-transfer process in photoexcited $BP(OH)_2$ in TMOS is presented in Figure 9. In this picture, the excited-state potential energy surface is sketched as a function of two vibrational coordinates, these being most likely typical of stretching and bending modes. The concerted process is thought to be assisted by the stretching mode (coordinate along the diagonal of the ground face) and the consecutive process is triggered by the bending mode (coordinate along either the *x*-or *y*-direction of the ground face). For the dienol-to-monoketo reaction in the two-step process, the activation energy is estimated to be 300 cm^{-1}, whereas the activation energy for the second step, the monoketo-to-diketo reaction (5 ps), is still unknown.

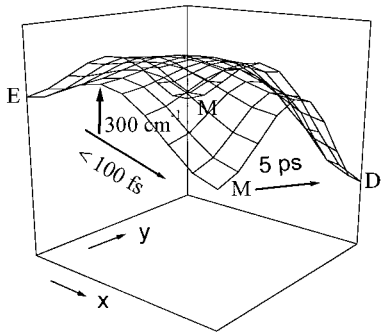

Figure 9. Sketch of excited-state potential energy surface for $BP(OH)_2$ used to discuss the photoinduced double proton transfer. *E* is energy of initially excited dienol tautomer. The *x*- and *y*-coordinates are illustrative of the bending mode displacements, giving the minima representing the intermediate monoketo tautomer forms (labeled M), displacement along the diagonal is representative of the stretching mode coordinate eventually giving the diketo product (D).

In TMSPM, the $BP(OH)_2$ absorption is red-shifted by some 20 nm compared to the absorption in cyclohexane, and the 0−0 transition may hence be at an energy lower than 27 400 cm^{-1}. The value for V_0 obtained from the fit according to the simplified model is about 28 000 cm^{-1}. Thus, in TMSPM, the activation energy for the dienol-to-monoketo reaction becomes more similar to that in apolar liquid solution.

With the parameter values given above, the imaginary angular frequency for tunneling, $i\omega_{\ddagger} = (A/m)^{1/2}$, is calculated as 1.2×10^{15} s^{-1} for TMOS and as 2.1×10^{15} s^{-1} for TMSPM. As discussed above, the monoketo intermediate is formed within the laser pulse duration time of 100 fs. In this time interval, the system has passed the tunneling region and, depending on the width of the potential barrier, could readily have performed several virtual oscillations with a period of about 5 fs for TMOS and 3 fs for TMSPM, while being in the tunneling region.

As shown in Section 3c, for $BP(OH)_2$ in the TMSPM sol−gel glass the fluorescence transients could be followed as a function of temperature down to 5 K. No variation with temperature was found; in particular, the c_1/c_2 ratio did not show a temperature dependence. This result implies that the initially excited-state population in the dienol form is so short-lived before its branched decay into the monoketo and diketo forms that thermalization of this population before passing the barrier to the monoketo tautomer is of no importance and thus has no effect on the c_1/c_2 ratio. This is expected since the dienol excited-state lifetime is shorter than 100 fs and electron−phonon interactions are typically on a picosecond time scale.

From Figure 8, it is seen that at the higher excitation energies the c_1/c_2 ratio attains the limiting value of about 1.5 and 0.7 for $BP(OH)_2$ in TMOS and TMSPM sol−gel glasses, respectively. The limiting value for $BP(OH)_2$ in fluid cyclohexane solution was about 0.7 (ref 4). At first sight, one expects the limiting value to be 2 if the double proton transfer of $BP(OH)_2$ would not show any preference for either the one-step or the two-step mechanism and thus the statistical limit value of 2 would be obtained. This value was actually found experimentally when the excitation, at 267 nm, is possibly to the excited S_2 state.[4] However, in the present work, even when excitation is far above the barrier top at 28 000 cm^{-1}, a value for c_1/c_2 lower than that of the statistical limit is obtained, implying that in the relaxation processes leading to the formation of the monoketo and diketo tautomers an additional dark relaxation channel, competitive to the formation channels of the tautomers, is active. As a result, the statistical limit value for the yields of the monoketo and diketo products is not achieved. Intramolecular vibrational relaxation (IVR) is a very likely candidate for the additional radiationless decay process. However, the different limiting values for c_1/c_2 in the TMOS and TMSPM samples suggest also that coupling to the host material may influence the vibrational relaxation dynamics in photoexcited $BP(OH)_2$; coupling to the more rigid network in TMSPM is apparently more effective in the vibrational relaxation than the coupling to the layer of solvent molecules in TMOS.

Acknowledgment. This work was supported in part by The Netherlands Foundation for Chemical Research (SON) with the financial aid from The Netherlands Organization for Scientific Research (NWO). One of us (P.P.) gratefully acknowledges a Marie Curie Research Training Grant of the EC Training and Mobility of Researchers (TMR) Program.

References and Notes

(1) Chachisvillis, M.; Fiebig, T.; Douhal, A.; Zewail, A. Z. *J. Phys. Chem.* **1998**, *102*, 669.
(2) Marks, D.; Zhang, H.; Glasbeek. M.; Borowicz, P.; Grabowska, A. *Chem. Phys. Lett.* **1997**, *275*, 370.
(3) Benderskii, V. A.; Goldanskii, V. I. *Int. Rev. Phys. Chem.* **1992**, *11*, 1.
(4) Marks, D.; Prosposito, P.; Zhang, H.; Glasbeek, M. *Chem. Phys. Lett.* **1998**, *289*, 535.
(5) Douhal, A.; Kim, S. K.; Zewail, A. H.; *Nature* **1995**, *378*, 260.
(6) Zhang, H.; van der Meulen, P.; Glasbeek, M.; *Chem. Phys. Lett.* **1996**, *253*, 97.
(7) Chudoba, C.; Riedle, E.; Pfeiffer, M.; Elsaesser, T. *Chem. Phys. Lett.* **1996**, *263*, 622.
(8) Chudoba, C.; Lutgan, S.; Jentzsch, T.; Riedle, E.; Woerner, M.; Elsaesser, T. *Chem. Phys. Lett.* **1995**, *240*, 35.
(9) Barbara, P. F.; Brus, L. E.; Rentzepis, P. M. *J. Am. Chem. Soc.* **1980**, *102*, 5631.
(10) Douhal, A.; Fiebig, T.; Chachisvilis, M.; Zewail, A. H. *J. Phys. Chem. A* **1998**, *102*, 1657.
(11) Mitra, S.; Tanai, N. *Chem. Phys. Lett.* **1998**, *282*, 391.
(12) Smith, T. P.; Zaklika, K. A.; Thakur, K.; Walker, G. C.; Tominaga, K.; Barbara, P. F. *J. Phys. Chem.* **1991**, *95*, 10465.
(13) Syage, J. A. *J. Phys. Chem.* **1995**, *99*, 5772.
(14) Kasha, M. *J. Phys. Chem.* **1991**, *95*, 10215.
(15) Barbara, P. F.; Walker, G. C.; Smith, T. P. *Science* **1992**, *256*, 975.
(16) Douhal, A.; Lahmani, F.; Zewail, A. H. *Chem. Phys.* **1996**, *207*, 477.
(17) Douhal, A.; Lahmani, F.; Zehnacker-Rentien, A.; Amat, F. *J. Phys. Chem.* **1994**, *98*, 12198.
(18) Share, P.; Pereira, M.; Sarisky, M.; Repinec, S.; Hochstrasser, R. M. *J. Lumin.* **1991**, *48* and *49*, 204.
(19) Elsaesser, T. In *Femtosecond Chemistry*; Marz, J., Wöster, L., Eds.; VCH: Germany, 1995; p 563.
(20) Pfeiffer, M.; Lenz, K.; Lau, A.; Elsaesser, T. *J. Raman Spectrosc.* **1995**, *26*, 607.
(21) Douhal, A. *Science* **1997**, *276*, 221.
(22) Bulska, H. *Chem. Phys. Lett.* **1983**, *98*, 398.
(23) Bulska, H.; Grabowska, A.; Grabowski, Z. R. *J. Lumin.* **1986**, *35*, 189.
(24) Bulska, H. *J. Lumin.* **1988**, *39*, 293.
(25) Kaschke, M.; Rentsch, S.; Opfermann, J. *Laser Chem.* **1988**, *8*, 377.
(26) Sepiol, J.; Bulska, H.; Grabowska, A. *Chem. Phys. Lett.* **1987**, *140*, 607.
(27) Eyal, M.; Reisfeld, R.; Chernyak, V.; Kaczmarek, L.; Grabowska, A. *Chem. Phys. Lett.* **1991**, *176*, 531.
(28) Levy, D. *J. Non-Cryst. Solids* **1992**, *147* and *148*, 508.
(29) Reisfeld, R. *Opt. Mater.* **1994**, *4*, 1.
(30) Avnir, D. *Acc. Chem. Res.* **1995**, *28*, 328.
(31) Sorek, Y.; Reisfeld, R.; Finkelstein, I.; Ruschin, S. *Appl. Phys. Lett.* **1995**, *66*, 1169.
(32) Shamrakov, D.; Reisfeld, R. *Opt. Mater.* **1994**, *4*, 103.
(33) Zhang, Y.; Cui, Y. P.; Wung, C. J.; Prasad, P. N.; Burzynski, R. *Proc. SPIE Int. Soc. Opt. Eng.* **1991**, *1560*, 264.
(34) Avnir, D.; Levy, D.; Reisfeld, R. *J. Phys. Chem.* **1984**, *88*, 5956.
(35) Fujii, T.; Ishii, A.; Anpo, M. *J. Photochem. Photobiol., A* **1990**, *54*, 231.
(36) Reisfeld, R. *J. Non-Cryst. Solids* **1990**, *121*, 254.
(37) Levy, D. *New J. Chem.* **1994**, *18*, 1073.
(38) Jin, T.; Inoue, S.; Tsutsumi, S.; Machida, K.; Adachi, G. *J. Non-Cryst. Solids* **1998**, *223*, 123.

(39) Casalboni, M.; Senesi, R.; Prosposito, P.; De Matteis, F.; Pizzoferrato, R. *Appl. Phys. Lett.* **1997**, *70*, 2969.
(40) De Rossi, U.; Daehne, S.; Reisfeld, R. *Chem. Phys. Lett.* **1996**, *251*, 259.
(41) McKiernan, J.; Pouxviel, J. C.; Dunn, B.; Zink, J. I. *J. Phys. Chem.* **1989**, *93*, 2129.
(42) Matsui, K.; Matsuzuka, T.; Fujita, H. *J. Phys. Chem.* **1989**, *93*, 4991.
(43) Pouxviel, J. C.; Dunn, B.; Zink, J. I. *J. Phys. Chem.* **1989**, *93*, 2134.
(44) Casalboni, M.; De Matteis, F.; Ferone, V.; Prosposito, P.; Senesi, R.; Pizzoferrato, R.; Bianco, A.; De Mico, A. *Chem. Phys. Lett.*, submitted for publication.
(45) Schmidt, H. In *Sol-Gel Science and Technology*; Aegerter, M. A., Souza, D. F., Jafelicci, M., Jr., Zanotto, E. D., Eds.; World Scientific: Singapore, 1989; pp 432−469.
(46) Schmidt, H.; Seiferling, B.; Phillip, G.; Deichmann, K. In *Ultrastructure Processing of Advanced Ceramics*; Mackenzie, J. D., Ulrich, D., Eds.; Wiley-Interscience: New York, 1988; p 651.
(47) Brinker, C. J.; Scherer, G. W. *The Physics and Chemistry of Sol-gel Processing*; Academic Press: New York, 1990.
(48) Hench, L. L.; West, J. K. *Chem. Rev.* **1990**, *90*, 33.
(49) Middelhoek, E. R.; van der Meulen, P.; Verhoeven, J. W.; Glasbeek, M. *Chem. Phys.* **1995**, *198*, 573.
(50) Zhang, H.; Jonkman, A. M.; van der Meulen, P.; Glasbeek, M. *Chem. Phys. Lett.* **1994**, *224*, 551.
(51) van der Meulen, P.; Zhang, H.; Jonkman, A. M.; Glasbeek, M. *J. Phys. Chem.* **1996**, *100*, 5367.
(52) Kahlow, M. A.; Jarzeba, W.; Dubrull, T. P.; Barbara, P. F. *Rev. Sci. Instrum.* **1988**, *59*, 1098.
(53) Maroncelli, M.; Fleming, G. R. *J. Chem. Phys.* **1987**, *86*, 6221.
(54) Bell, R. P. *The Tunnel Effect in Chemistry*; Chapman and Hall: New York, 1980.
(55) Sobolewski, A. L.; Adamowicz, L. *Chem. Phys. Lett.* **1996**, *252*, 33.